PhD Dissertation Defense

Higgs boson cross section measurements in the diphoton decay channel in proton-proton collisions at $\sqrt{s} = 13\,\mathrm{TeV}$ using the ATLAS detector at the LHC

Ivan Pogrebnyak

Adviser: Joey Huston

December 4, 2020

Introduction

- Higgs boson is the central, but only most recently discovered, element of the Standard Model.
  - Discovered at the LHC in 2012
- Post-discovery efforts concentrate on measurements of properties.
- Cross section measurements in $H \to \gamma\gamma$ channel
  - Counting analysis
  - Higgs events cannot be identified individually, only statistically counted

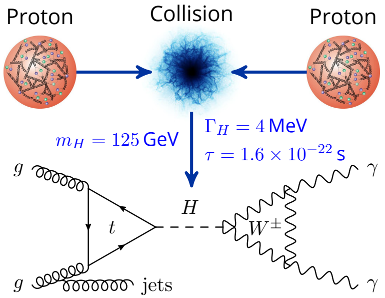

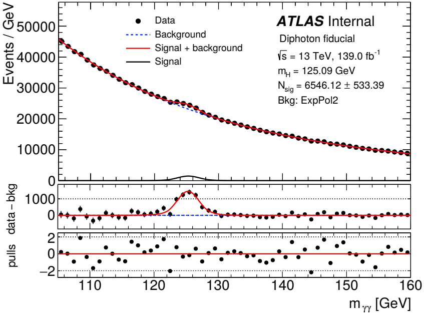

Measured number of events $\to$
Cross section $\to$
Integrated luminosity $\to$

$$\sigma = \frac{N_{\text{sig}}}{\int L\,dt} \tag{1}$$

N particles per beam bunch $\to$
Luminosity $\to$
Effective beams overlap area $\to$

$$L = \frac{N_1 N_2 f_{\text{b}}}{A_{\text{eff}}} \tag{2}$$

$\leftarrow$ Frequency of bunch crossings

Outline

- Theory
  - Standard Model of particle physics
  - Quantum Field Theory
  - Higgs mechanism
  - Higgs boson production
- Experiment
  - Large Hadron Collider
  - ATLAS detector
- $H \to \gamma\gamma$ cross section measurements
  - Analysis strategy and methods
  - Signal extraction
  - Uncertainties
  - Results

Standard Model of particle physics

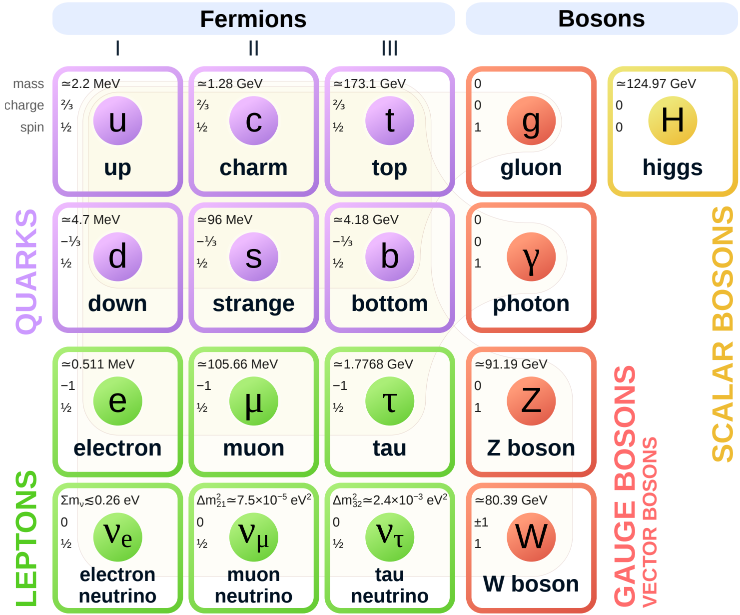

Quantum Field Theory

- Principle of least action,

$$\mathcal{S} = \int d^4\mathrm{x}\, \mathcal{L}\big(\phi(\mathrm{x}), \dot{\phi}(\mathrm{x})\big). \tag{3}$$

- Quantum mechanics
  - Canonical quantization
  - Path integral formulation
- Special relativity
- Symmetry $\Leftrightarrow$ conservation laws
- Gauge fields

$$\overbrace{\underbrace{U(1)_Y}_{\text{Weak hypercharge}} \times \underbrace{SU(2)_\mathrm{L}}_{\text{Weak isospin}}}^{\text{Electroweak}} \times \overbrace{\underbrace{SU(3)_c}_{\text{Color}}}^{\text{Strong}} \tag{4}$$

Role of the Higgs field

- Gauge boson masses via electroweak symmetry breaking
  - Naive mass terms for gauge bosons break gauge symmetry of the Lagrangian
  - This is the problem solved by the Higgs mechanism
- Fermion masses via Yukawa coupling
  - Naive mass terms for fermions don't work for exclusively left-handed weak interaction
  - Explanation via coupling to the Higgs field consistent with observations

Implications:

- Fundamental status of the Standard Model
- Stability of the electroweak vacuum
- A potential probe for physics beyond the Standard Model

Higgs mechanism analogy

- In 1993, UK Science Minister, Waldegrave, offered a bottle of vintage champagne for a lay-person description of the Higgs boson.
- Animated version: https://www.symmetrymagazine.org/article/september-2013/famous-higgs-analogy-illustrated

[1, 2]

Higgs mechanism analogy

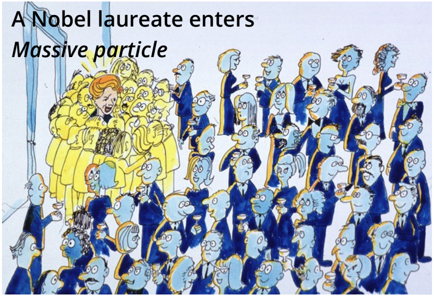

[1, 2]

Higgs mechanism analogy


Physicists at a conference
Higgs field

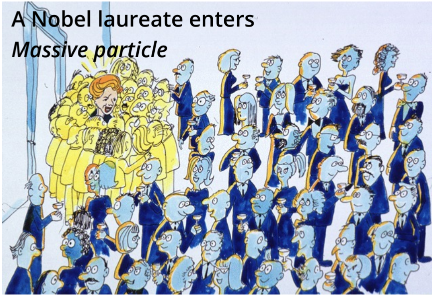
A Nobel laureate enters
Massive particle


A rumor is started
Higgs field excitation

[1, 2]

Higgs mechanism analogy

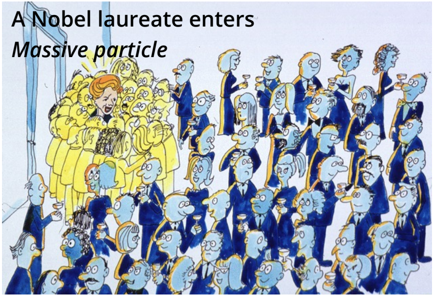

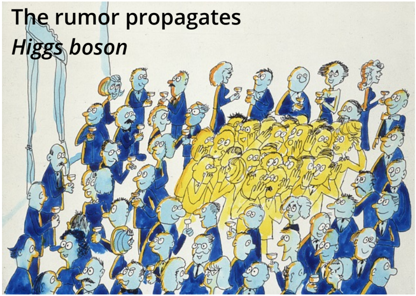

[1, 2]

Higgs mechanism for $U(1)$

- Simplest massless gauge field, $U(1)$, i.e. photon:

$$\mathcal{L} = -\frac{1}{4} F_{\mu\nu} F^{\mu\nu}, \quad F_{\mu\nu} = \partial_\mu A_\nu - \partial_\nu A_\mu. \tag{5}$$

- Naive mass term, $\frac{1}{2} m^2 A_\mu A^\mu$, breaks gauge invariance.
- Add a complex scalar field, ϕ:

$$\mathcal{L} = -\frac{1}{4} F_{\mu\nu} F^{\mu\nu} + (D_\mu \phi)^\dagger (D^\mu \phi) - \mu^2 \phi^\dagger \phi - \lambda (\phi^\dagger \phi)^2. \tag{6}$$

- Covariant derivative (to preserve gauge invariance):

$$D_\mu = \partial_\mu - igA_\mu. \tag{7}$$

- Gauge transformation:

$$A_\mu(x) \to A_\mu(x) - \partial_\mu \alpha(x), \quad \phi(x) \to \phi(x) e^{-i\alpha(x)}. \tag{8}$$

Higgs mechanism for $U(1)$

$$V(\phi) = \mu^2\phi^\dagger\phi + \lambda(\phi^\dagger\phi)^2$$

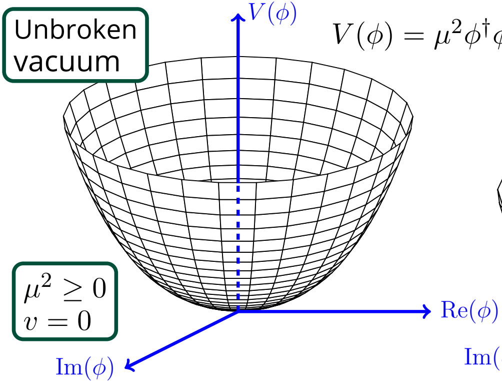

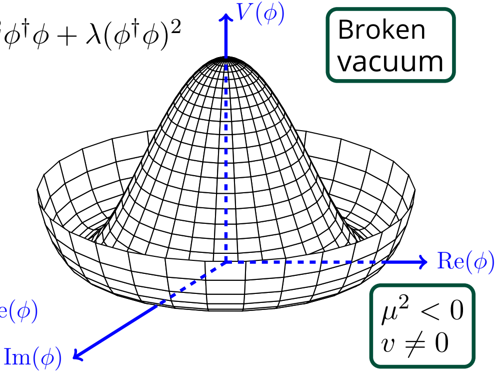

- Parametrize the scalar field around the minimum:

$$\phi = \frac{v+h}{\sqrt{2}}\, e^{i\chi/v}, \quad \langle\phi\rangle = \sqrt{\frac{-\mu^2}{2\lambda}} = \frac{v}{\sqrt{2}}. \tag{9}$$

- Massive Higgs boson, h, $m_h = \sqrt{2}\mu = \sqrt{2\lambda}v$.
- Massless Goldstone boson, χ, is *eaten* by the gauge field, A_μ.

Higgs mechanism for $U(1)$

- The Lagrangian becomes:

$$
\begin{aligned}
\mathcal{L} = &-\frac{1}{4}F_{\mu\nu}F^{\mu\nu} && \text{the original gauge field} \\
&+\frac{g^2v^2}{2}A_\mu A^\mu && \text{the acquired mass term} \\
&- gvA_\mu\partial^\mu\chi && \text{can be removed via unitary gauge} \\
&+\frac{1}{2}\left(\partial_\mu h\partial^\mu h - 2\mu^2h^2\right) && \text{massive Higgs boson} \\
&+\frac{1}{2}\partial_\mu\chi\partial^\mu\chi && \text{non-interacting Goldstone boson} \\
&+\text{(interaction terms)} && \text{possible couplings to other fields}
\end{aligned}
$$

- For $U(1)\times SU(2)$, ϕ is a complex doublet with 4 degrees of freedom, 3 of which are consumed by the electroweak bosons.

Higgs production channels

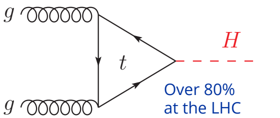

(a) Gluon-gluon Fusion (ggF).

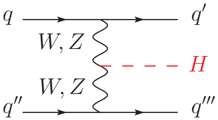

(b) Vector Boson Fusion (VBF).

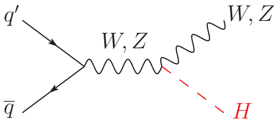

(c) Associated production with weak bosons at tree level (WH, ZH).

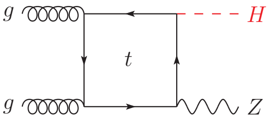

(d) Associated production with weak bosons at loop level (ZH).

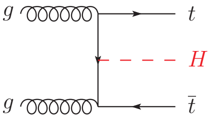

(e) Associated production with heavy quarks (bbH, ttH).

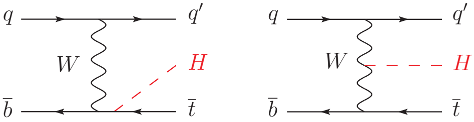

(f) Associated production with single top quark (tH).

[3]

Additional QCD radiation

- Most event have at least some soft gluon radiation
  - Higgs $p_\mathrm{T} > 0$
  - $\sim$ 1/3 events with $\geq$1 jet
- Large NLO corrections
  - Lack of QCD radiation requires full color-charge cancelation of 2 color octets in the initial state
- Sudakov peak in low-p_T region sensitive to resummation
- Coupling
  - Effective coupling to gluons
  - Yukawa coupling to quarks
- High p_T region has much larger signal/background ratio
- Top quark mass effects

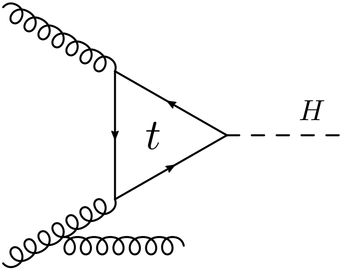

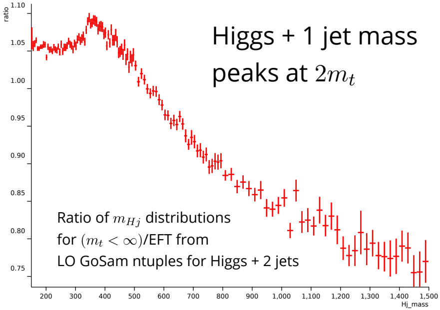

Higgs decay channels

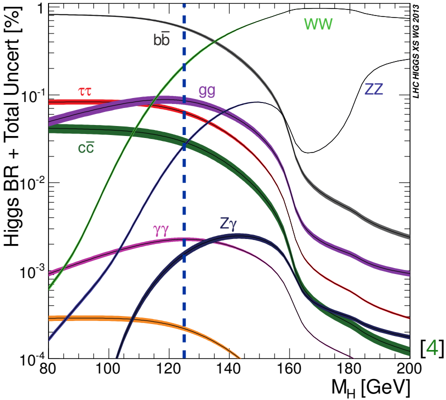

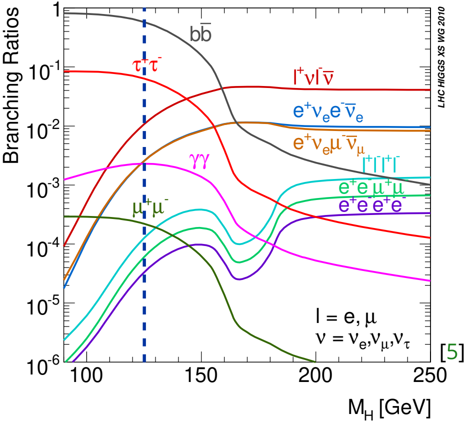

Discovery channels, 2012 [6, 7]:

- $\boxed{H \to \gamma\gamma}$
- $H \to ZZ^* \to 4\ell$

Recently accessible channels:

- $H \to b\bar{b}$, 2018 [8]
- $H \to \tau\bar{\tau}$, 2019 [9]
- $H \to \mu\bar{\mu}$, 2020 [10, 11] $(2\,\sigma)$

*Other channels inaccessible due to large background

Background process

- QCD diphoton production

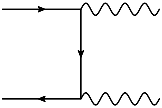

(a) $q\bar{q} \to \gamma\gamma$ @ LO

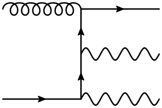

(b) $qg \to \gamma\gamma$ @ NLO

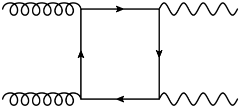

(c) $gg \to \gamma\gamma$ @ NLO

- Simple smoothly falling background

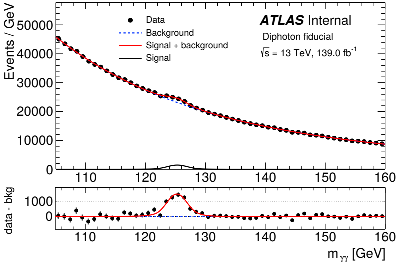

(d) Inclusive event selection

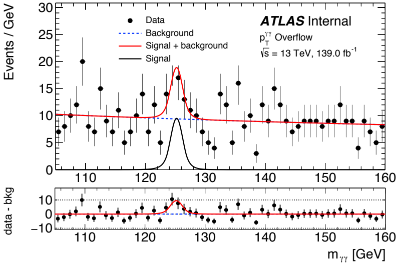

(e) $p_{\mathrm{T}}^{\gamma\gamma} > 350$ GeV

- Signal/Background ratio increases at high $p_{\mathrm{T}}^{\gamma\gamma}$

Large Hadron Collider

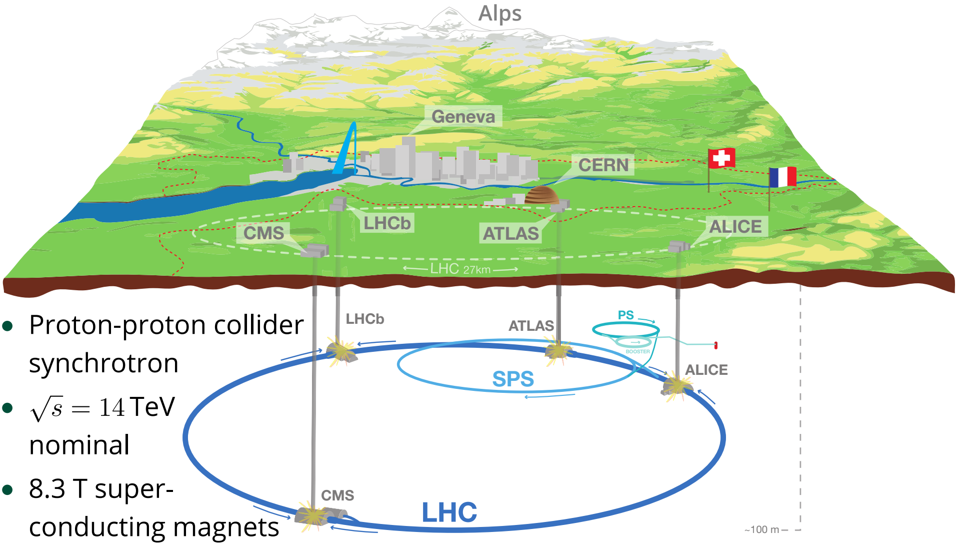

- Proton-proton collider synchrotron
- $\sqrt{s} = 14$ TeV nominal
- 8.3 T super-conducting magnets
- 27 km circumference

[12]

ATLAS detector

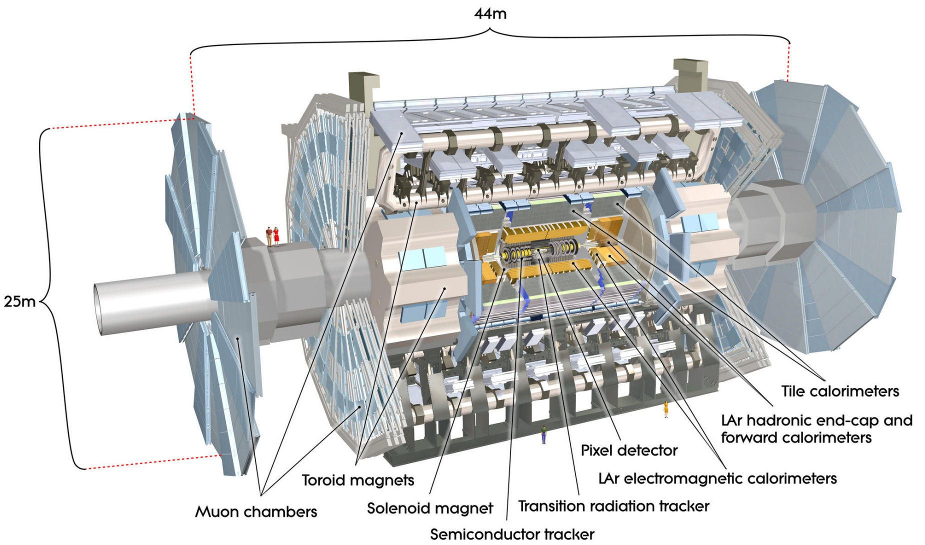

[13]

Detection of particles

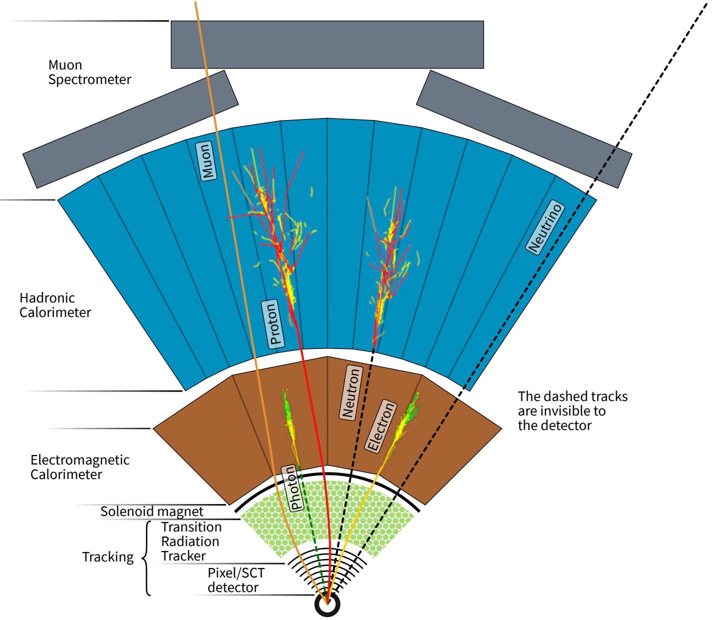

[14]

Hadronic Tile Calorimeter

- MSU historically involved in TileCal
- I participated in development and testing of the Phase-II upgrades
  - My ATLAS membership project
  - FPGA firmware for on-detector electronics
  - HV and LV power control and monitoring

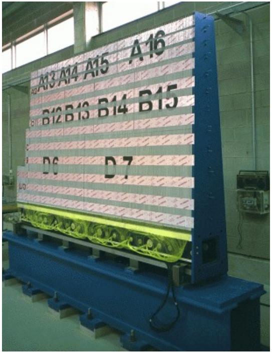

Visiting ATLAS detector in summer of 2019

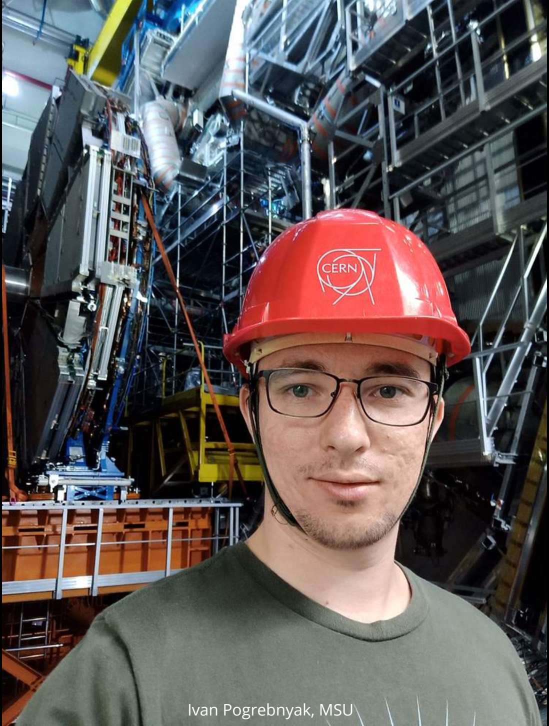

Analysis strategy

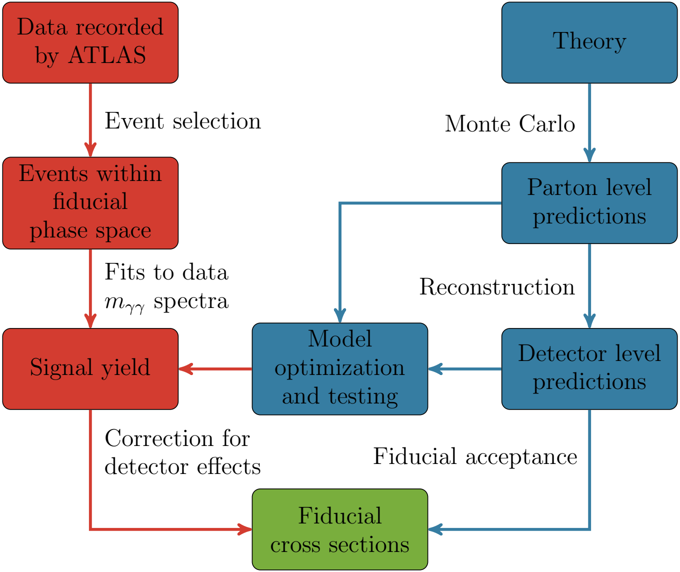

Event selection

Photons:

- $p_{\mathrm{T}} > 25$ GeV
- $|\eta| < 2.37$, excluding $1.37 < |\eta| < 1.52$
- $p_{\mathrm{T}}/m_{\gamma\gamma} > 0.35(0.25)$ for (sub)leading photon
- $\Delta R > 0.2$ isolation

$$p_{\mathrm{T}} = \sqrt{p_x^2 + p_y^2}$$

$$\Delta R = \sqrt{\Delta\eta^2 + \Delta\phi^2}$$

$$\eta = -\log\tan\frac{\theta}{2}$$

Diphoton:

- $m_{\gamma\gamma} \in [105, 160]$ GeV
- Two leading jets
- Primary vertex corrected

Jets (AntiKt4):

- $p_{\mathrm{T}} > 30$ GeV
- $|\eta| < 4.4$
- JVT, fJVT (reduce pileup)
- $\Delta R > 0.4$ to photons
- $\Delta R > 0.2$ to electrons

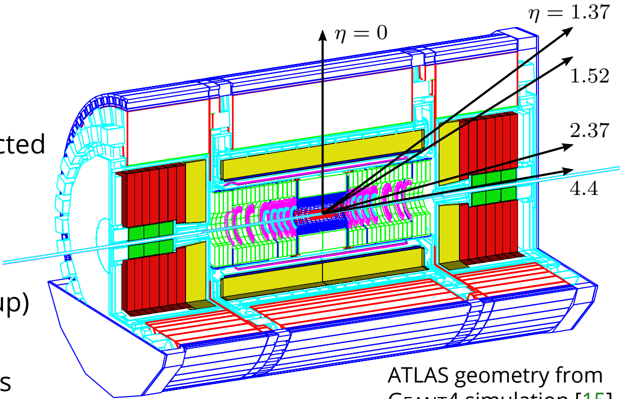

ATLAS geometry from GEANT4 simulation [15]

Dataset

Year	Period	Luminosity	Luminosity uncertainty	Number of events
2015	D–J	$3.2\,\mathrm{fb}^{-1}$	2.1%	28 741
2016	A–L	$32.9\,\mathrm{fb}^{-1}$	2.2%	283 178
2017	B–K	$44.3\,\mathrm{fb}^{-1}$	2.4%	370 086
2018	B–Q	$58.5\,\mathrm{fb}^{-1}$	2.0%	496 082
Total		$139.0\,\mathrm{fb}^{-1}$	1.7%	1 178 087

Selection efficiency:

- Relative to all recorded events: 0.00686%
- Relative to events passing diphoton trigger: 0.387%

Simulated event samples

Monte Carlo event generators

- Provide theoretical cross section predictions
- Used in preparatory and optimization studies
- Correction for detector effects, unfolding
- Assessment of uncertainties

Process	Generator	PS	PDF	ME order	Normalisation order	$\sigma \times$ BR, fb
ggF	Powheg NNLOPS	Pythia8	PDF4LHC15	NNLO + NLL(QCD)	N^{3}LO(QCD) + NLO(EW)	110
VBF	Powheg-Box	Pythia8	PDF4LHC15	NLO(QCD)	approx. NNLO(QCD) + NLO(EW)	8.58
W^+H	Powheg-Box	Pythia8	PDF4LHC15	NLO(QCD)	NNLO(QCD) + NLO(EW)	1.90
W^-H	Powheg-Box	Pythia8	PDF4LHC15	NLO(QCD)	NNLO(QCD) + NLO(EW)	1.21
$q\bar{q} \to ZH$	Powheg-Box	Pythia8	PDF4LHC15	NLO(QCD)	NNLO(QCD) + NLO(EW)	1.73
$gg \to ZH$	Powheg-Box	Pythia8	PDF4LHC15	LO(QCD)	NLO(QCD) + NLO(EW)	0.28
$t\bar{t}H$	Powheg-Box	Pythia8	PDF4LHC15	NLO(QCD)	NLO(QCD) + NLO(EW)	1.15
$b\bar{b}H$	Powheg-Box	Pythia8	PDF4LHC15	NLO(QCD)	5FS (NNLO), 4FS (NLO)	1.10
WtH	aMC@NLO	Pythia8	CT10 NLO	NLO(QCD)	4FS(LO)	0.034
tHq	aMC@NLO	Pythia8	CT10 NLO	NLO(QCD)	5FS(NLO)	0.169
$\gamma\gamma$	Sherpa	Sherpa	CT10	NLO(QCD)	NLO(QCD)	19.2×10^3

Event simulation stages

- Parton level
  - Only matrix element calculation

- Particle level — “Truth”
  - Hadronic and electromagnetic showers
  - Hadronization
  - Hadronic decays

- Full simulation — “Reco”
  - Detector simulation
    - Full sim for signal processes
    - Fast sim for background
  - Same reconstruction algorithms as for data
    - Tracking
    - Jet clustering

Measured observables

- 4 fiducial categories
  - VBF, Leptons, Missing transverse energy, ttH
- 30 differential variables
  - p_T, y, Δy, $\Delta\phi$, m
- Higgs boson kinematics
  - $p_\mathrm{T}^{\gamma\gamma}$, $\left|\Delta y_{\gamma\gamma}\right|$, $p_\mathrm{T}^{\gamma\gamma j}$, $m_{\gamma\gamma j}$, $m_{\gamma\gamma jj}$
- Jet activity
  - p_T^{j}, N_jets (exclusive and inclusive), H_T, m_{jj}
- Spin, charge conjugation, and parity
  - $\left|\cos\theta^*\right|$, $\Delta\phi_{jj}$
- Couplings & production modes
  - VBF: $|\Delta y_{jj}|$, $\Delta\phi_{jj}$, $|\Delta y_{\gamma\gamma,jj}|$, $|\Delta\phi_{\gamma\gamma,jj}|$
  - ggF: $p_\mathrm{T}^{\gamma\gamma}$, $p_\mathrm{T}^{\gamma\gamma j}$, $m_{\gamma\gamma j}$, $\left|y_{\gamma\gamma}\right|$

Analysis strategy

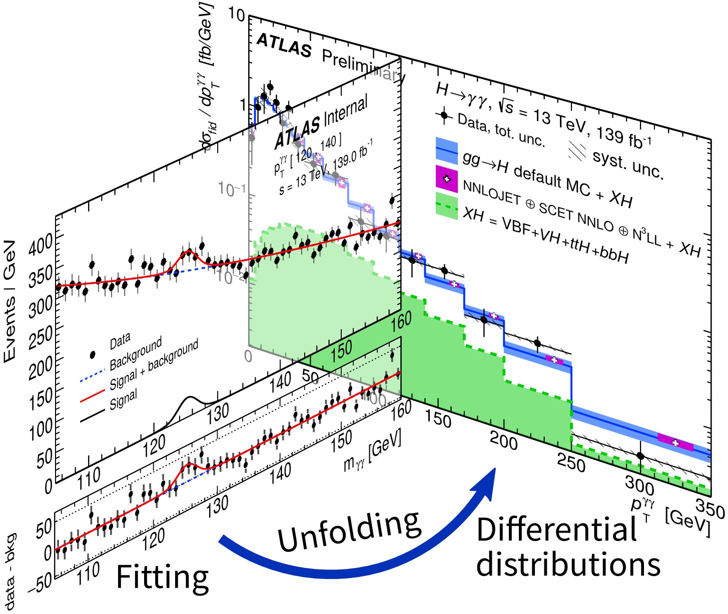

Binning

Binning F-test Events GP test Links Git repos

H→γγ binning estimator

Luminosity: 140.429 ifb

pT_yy ▾ 0 5 10 15 20 25 30 35 45 60 80 100 120 Rebin (0.72 sec)

☑ click row to show backround fit ☐ show uncertainties

bin	[121,129] sig	[105,121] L bkg	[129,160] R bkg	[121,129] bkg	signif s/√(s+b)	signif Cowan	s/(s+b)	reco purity
[0,5)	259.68	34526	22124	10675.40	2.48	2.50	2.37%	84.32%
[5,10)	553.63	65599	41479	20339.20	3.83	3.86	2.65%	82.25%
[10,15)	593.88	70883	45007	22026.50	3.95	3.98	2.63%	81.39%
[15,20)	546.23	64439	42372	20210.40	3.79	3.83	2.63%	81.15%
[20,25)	478.96	54807	37674	17571.00	3.57	3.60	2.65%	81.05%
[25,30)	412.52	45083	32569	14862.10	3.34	3.37	2.70%	80.93%
[30,35)	353.40	37408	27564	12409.90	3.13	3.16	2.77%	80.64%
[35,45)	562.52	56874	44064	19434.20	3.98	4.02	2.81%	89.17%
[45,60)	589.72	54366	45195	19018.70	4.21	4.25	3.01%	91.92%
[60,80)	497.54	40512	36157	14740.20	4.03	4.08	3.27%	92.99%
[80,100)	310.40	18582	20851	7717.91	3.46	3.51	3.87%	92.58%
[100,120)	202.03	8867	10932	3664.58	3.25	3.31	5.22%	92.21%
[120,140)	141.21	4650	5822	1952.00	3.09	3.16	6.75%	91.79%
[140,170)	141.56	3335	4559	1480.12	3.52	3.62	8.73%	93.40%
[170,200)	87.85	1503	2202	685.42	3.16	3.29	11.36%	92.88%
[200,250)	80.51	1058	1567	479.03	3.40	3.58	14.39%	94.51%
[250,350)	57.19	593	849	254.88	3.24	3.46	18.33%	95.76%
[350,∞)	23.22	157	272	84.36	2.24	2.42	21.58%	96.94%

sig - number of signal events, taken from Monte Carlo.

bkg - number of background events in the signal region, estimated from data sidebands.

signal systematic uncertainty - square root of sum of MC event weights.

Background in the signal region is estimated by a fit to the *m_yy* sidebands.
The fit is done using a weighted linear least-squares algorithm.
A second degree polynomial is fit to *logs* of bin counts.

The second significance column labelled Cowan is calculated using equation $\sqrt{2[(s+b)\log(1+s/b)-s]}$.
See the "Discovery significance ..." note by Glen Cowan.

Year	Lumi [ifb]	MC	merge factor
15,16	36.184	mc16a	0.257668
17	44.307	mc16d	0.315512
18	59.938	mc16e	0.426821

MxAOD files [show]

Reco migration [hide]

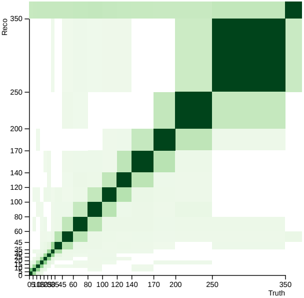

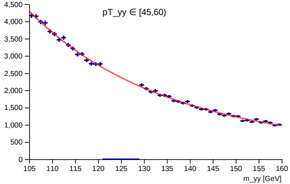

χ^2 = 50.6998 ndf = 44
p_0 = 1.254e+01
p_1 = -4.818e-02
p_2 = 7.999e-05

cov:
6.145e-02 -9.592e-04 3.679e-06
-9.592e-04 1.501e-05 -5.771e-08
3.679e-06 -5.771e-08 2.224e-10

Signal extraction

- Statistical model:
  - Function fit (regression)
  - Signal + Background

- Extended unbinned likelihood fit:

$$L_i \left(m_{\gamma\gamma} \middle| \nu_i^{\text{sig}}, \nu_i^{\text{bkg}} \right) = \frac{e^{-\nu_i}}{n_i!} \prod_j^n \left[\nu_i^{\text{sig}} \mathcal{S}\left({m_{\gamma\gamma}}^j \middle| \boldsymbol{\theta}_i^{\text{sig}} \right) + \nu_i^{\text{bkg}} \mathcal{B}\left({m_{\gamma\gamma}}^j \middle| \boldsymbol{\theta}_i^{\text{bkg}} \right) \right]$$

- $-2 \log \sum_i L_i$ is minimized
  - Sum runs over all bins in the distribution for a given variable
  - Minuit minimization algorithm via RooFit

Signal model

- Double-sided Crystal Ball function

$$\mathcal{S}(t) = \mathcal{N}_\mathrm{s} \cdot \begin{cases} e^{-t^2/2} & \text{if } \; -\alpha_\mathrm{L} \le t \\ e^{-\alpha_\mathrm{L}^2/2} \left[\left(R_\mathrm{L} - \alpha_\mathrm{L} - t \right) / R_\mathrm{L} \right]^{-n_\mathrm{L}} & \text{if } \; t < -\alpha_\mathrm{L}, \\ e^{-\alpha_\mathrm{H}^2/2} \left[\left(R_\mathrm{H} - \alpha_\mathrm{H} + t \right) / R_\mathrm{H} \right]^{-n_\mathrm{H}} & \text{if } \; t > \alpha_\mathrm{H}, \end{cases}$$

$$t = (m_{\gamma\gamma} - \mu)/\sigma, \quad R = n/\alpha$$

- Parameters $\mu, \sigma, \alpha_L, \alpha_H, n_L, n_H$ fixed from fits to MC.
- Normalization (number of signal events) fitted to data.
- Additional nuisance parameters modifying μ and σ propagate uncertainties from photon reconstruction

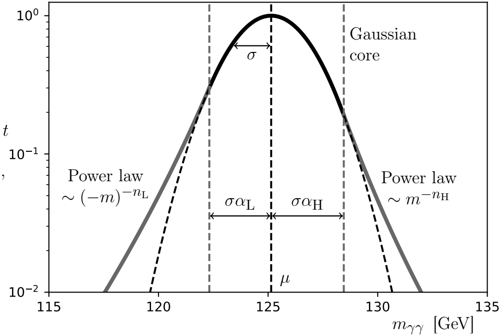

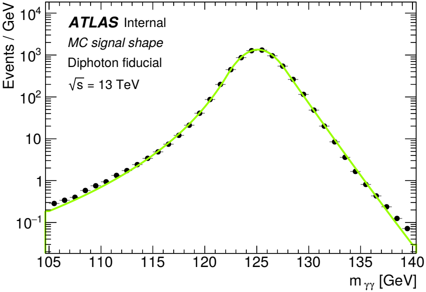

Background model

$$\texttt{ExpPoly}_N(x) = \exp\left(\sum_{n=0}^{N} a_n x^n\right),$$

$$\texttt{Bern}_N(x) = \sum_{n=0}^{N} c_n \binom{N}{n} x^n (1-x)^{N-n},$$

$$\texttt{Pow}_N(x) = \sum_{n=1}^{N} c_n x^{a_n}.$$

- Functional form selected for every bin using spurious signal studies
- Validated with F and likelihood ratio tests
- All parameters float in signal extraction fits

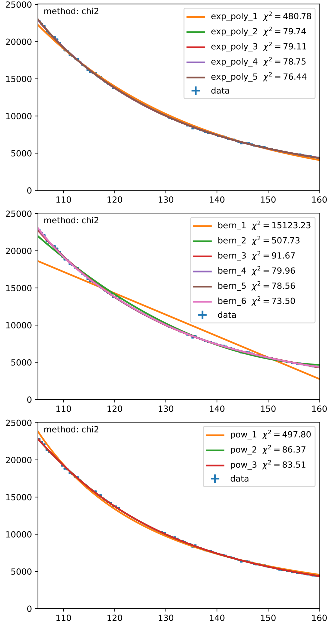

Spurious signal

- Signal + Background model fitted to background-only MC templates
  - $N_{\text{sp}} \pm n\Delta_{\text{sp}}$ must be less than 20% of the background uncertainty, δS, or
  - $N_{\text{sp}} \pm n\Delta_{\text{sp}}$ must be less than 10% of the expected number of signal events.
  - $n = \min(0, 1, 2)$ s.t. at least one background function passes
- Templates generated from background MC including detector simulation
  - Reweighted to include γj and jj contributions
  - Smoothed using Gaussian process regression

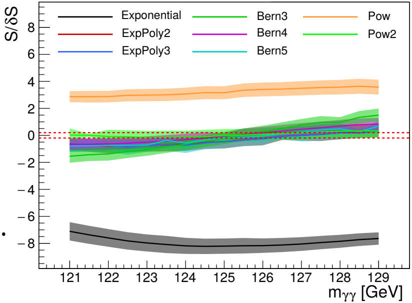

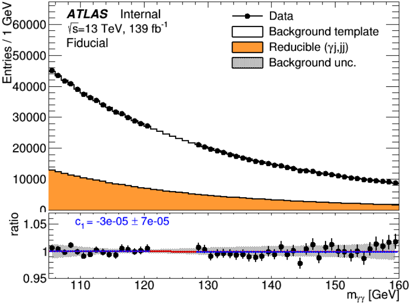

Background composition

- Irreducible background: QCD diphoton production, $\gamma\gamma$
  - $q\bar{q} \to \gamma\gamma$ at LO
  - $\{q\bar{q}, gg, gq\} \to \gamma\gamma$ at NLO
  - Fully simulated
- Reducible background
  - Jets misreconstructed as photons: $\gamma\gamma, \gamma j$
  - Added by reweighting

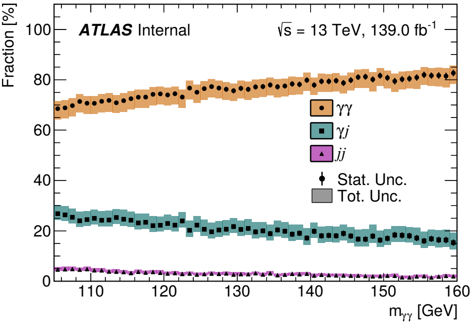

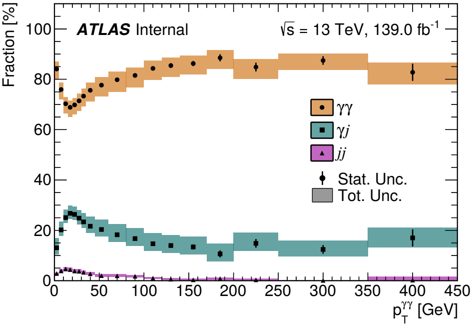

Goodness of fit tests

- F-test
  - $F = \dfrac{\frac{\chi_1^2 - \chi_2^2}{p_2 - p_1}}{\frac{\chi_2^2}{n - p_2}} = \dfrac{\Delta\chi^2}{\chi_2^2} \dfrac{\mathrm{ndf}_2}{\Delta\mathrm{ndf}}$
  - F distribution with $(\Delta\mathrm{ndf}, \mathrm{ndf}_2)$ degress of freedom
  - $P = \int_F^\infty f(t)\, dt$, probability that model 1 can fit at least as well as model 2.
  - Reject the null hypothesis at $P > 0.05$.

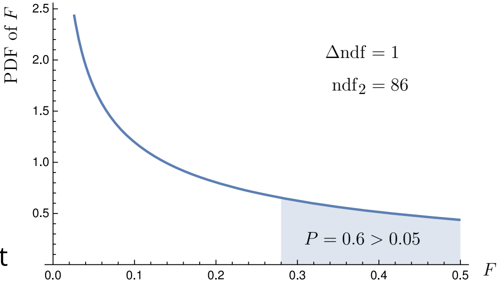

- Likelihood ratio test
  - $R = \log \dfrac{L_1}{L_2}$
  - χ^2 distribution with $\Delta\mathrm{ndf}$ degress of freedom
- Few categories (bins) fail.
  - Usually choose the function in the same family with one more degree of freedom.

Correction for detector effects

- Also known as unfolding or deconvolution
- Corrected cross section:

$$\sigma_i = \frac{\nu_i^{\text{sig}}}{c_i \times L} \tag{10}$$

- Bin-by-bin correction factors:

$$c_i = \frac{n_i^{\text{reco}}}{n_i^{\text{truth}}}, \quad n_i = \sum_s \frac{n_{s,i}}{N_s}\,\sigma_s^{\text{SM}} \tag{11}$$

s – MC sample, i – bin, n – event weights, $N_s = \sum_i n_{s,i}$

- Investigated more sophisticated methods:
  - Response matrix inversion
  - Bayesian iterative unfolding
  - Singular value decomposition (SVD) of the response matrix
  - Iterative, dynamically stabilized (IDS) unfolding

Photon energy scale and resolution

- Systematic uncertainty accounted for by introduction of nuisance parameters to signal extraction model

$$\mathcal{L} = \prod_{i \in \text{bins}} \mathcal{L}_i \prod_k \mathcal{C}_k(\theta_k), \quad \mathcal{C}_k(\theta_k) = \text{Gaus}(\theta_k; 0, 1) = \frac{1}{\sqrt{2\pi}} e^{-\theta_k^2/2} \tag{12}$$

- 1 symmetric variation: Higgs mass, $m_H = 125$ GeV from Run 1

$$\mu(\theta_{m_H}) = m_H^{\text{nom}} \cdot (1 + \delta_{m_H} \cdot \theta_{m_H}) \tag{13}$$

- 39 asymmetric variations: PES

$$\mu_i(\boldsymbol{\theta}^{\text{PES}}) = \mu_i^{\text{nom}} \cdot \prod_{k=1}^{N_{\text{PES}}} \left(1 + \delta_{k,i}^{\text{PES},\pm} \cdot \theta_k^{\text{PES}}\right) \tag{14}$$

- 9 asymmetric log-normal variations: PER

$$\sigma_i(\boldsymbol{\theta}^{\text{PER}}) = \sigma_i^{\text{nom}} \cdot \prod_{k=1}^{N_{\text{PER}}} \theta_k^{\text{PER}} \cdot \exp \sqrt{\ln\left(1 + \left(\delta_{k,i}^{\text{PER},\pm}\right)^2\right)} \tag{15}$$

Photon energy scale and resolution

- The effect of simultaneous variations of all photon calibrations on the diphoton mass spectrum

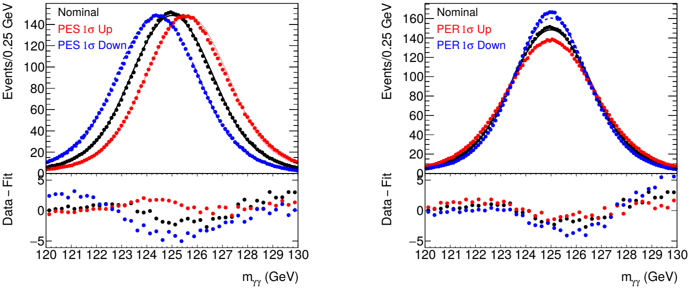

- Systematic MC samples generated for independent up and down variations of every single-photon uncertainty
- $\delta_{k,i}$ are diphoton uncertainties from source k for bin i derived by fitting the signal model to the systematic MC
- θ_k are the respective nuisance parameters, assumed equal for all bins

Inclusive fiducial uncertainties

Statistics	6.9%
Signal extraction syst.	7.9%
Photon energy scale & resolution	4.6%
Background modeling (spurious signal)	6.4%
Correction factor	2.6%
Pile-up modeling	2.0%
Photon identification efficiency	1.2%
Photon isolation efficiency	1.1%
Trigger efficiency	0.5%
Theoretical modeling	0.5%
Photon energy scale & resolution	0.1%
Luminosity	1.7%
Total	11.0%

Uncertainties for differential observables

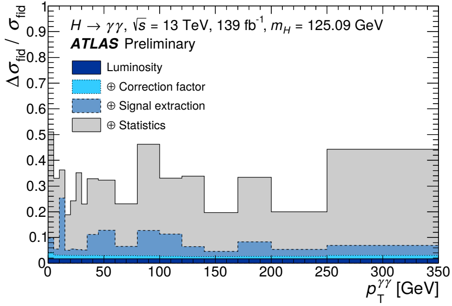

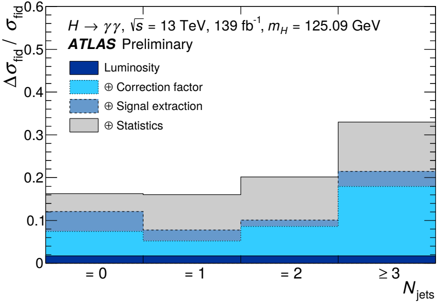

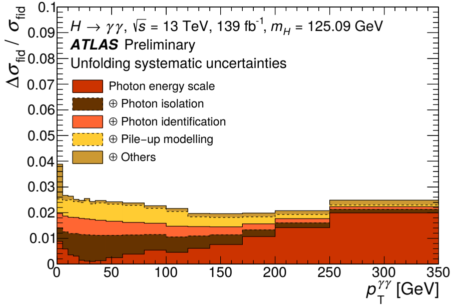

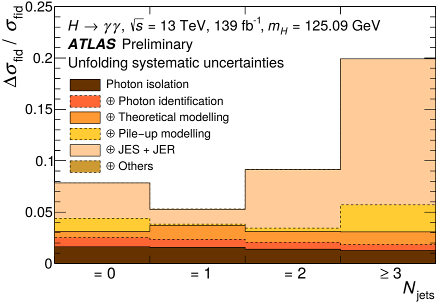

Results

- Measured inclusive fiducial cross section [16, 17]:

$$\sigma_{\text{fid}} = 65.2 \pm 4.5\,(\text{stat.}) \pm 5.6\,(\text{exp.}) \pm 0.3\,(\text{theory})\,\text{fb}$$
$$\approx 65.2 \pm 7.2\,\text{fb}$$

- Standard Model prediction [18]:

$$\sigma_{\text{fid}}^{\text{SM}} = 63.5 \pm 3.3\,\text{fb}$$

- Extrapolated total $pp \to H$ cross section [19]:
  - From $H \to \gamma\gamma$: $56.7^{+6.4}_{-6.2}$ pb
  - From $H \to ZZ^*$: $54.4^{+5.6}_{-5.4}$ pb
  - Combined: $55.4^{+6.1}_{-5.9}$ pb
  - SM: 55.6 ± 2.5 pb

Measured differential cross sections

$p_{\mathrm{T}}^{\gamma\gamma}$

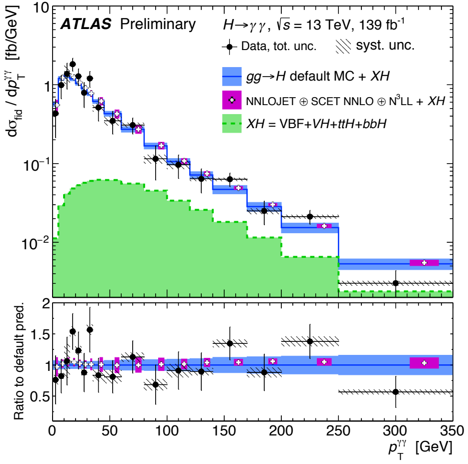

$p_{\mathrm{T}}^{j_1}$

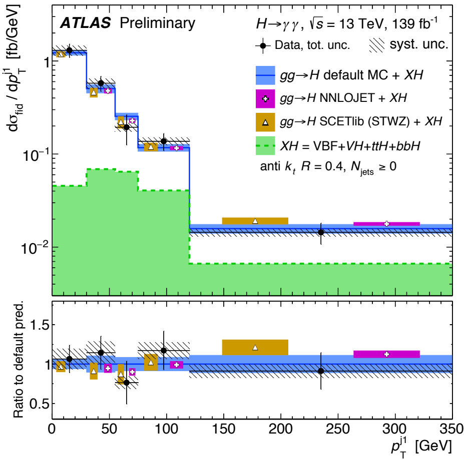

Measured differential cross sections

Jet multiplicity

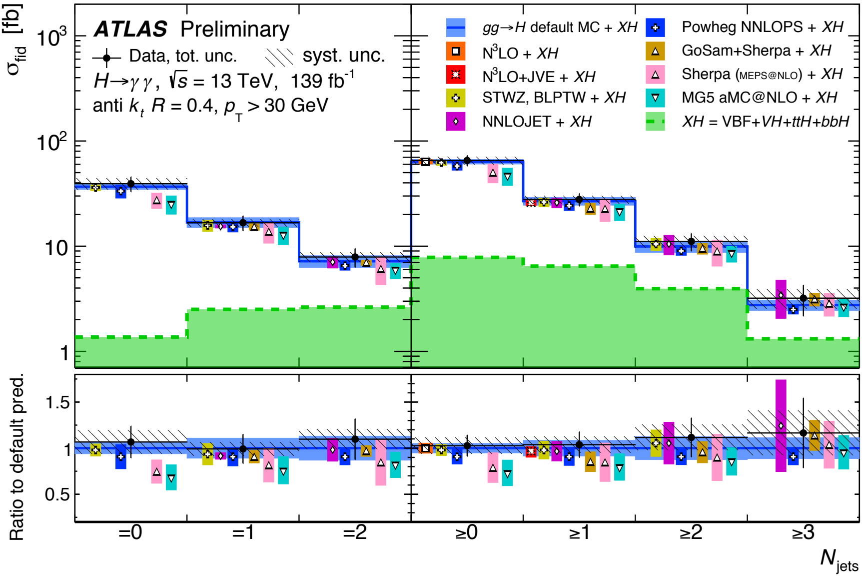

Publications

Luminosity	Data set	Publications
$3.2\,\mathrm{fb}^{-1}$	2015	ATLAS-CONF-2015-060 [20, 21]
$13.3\,\mathrm{fb}^{-1}$	2015–2016	ATLAS-CONF-2016-067 [22, 23]
$36.1\,\mathrm{fb}^{-1}$	2015–2016	ATLAS-CONF-2017-045, HIGG-2016-21 [24–26]
$79.8\,\mathrm{fb}^{-1}$	2015–2017	ATLAS-CONF-2018-028 [27, 28]
$139.0\,\mathrm{fb}^{-1}$	2015–2018	ATLAS-CONF-2019-029 [16, 17]

- A full Run 2 publication is being prepared.

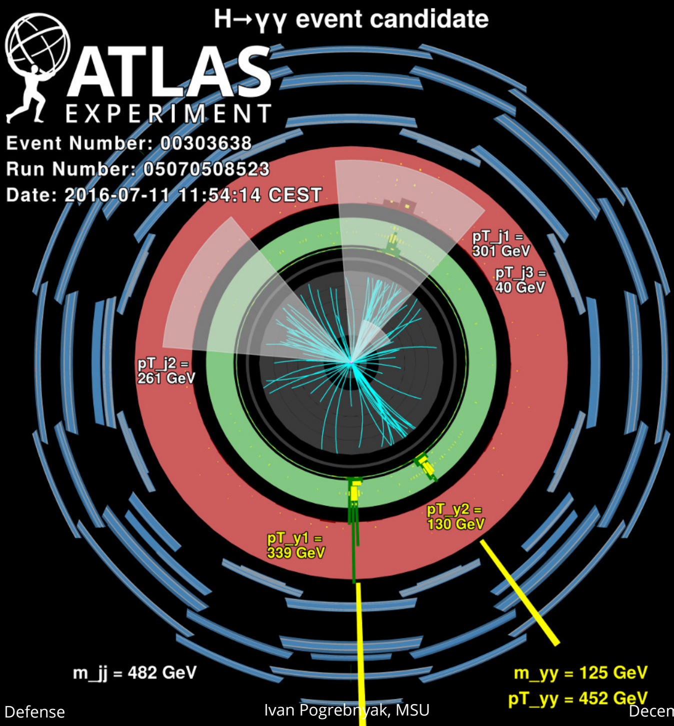

H→γγ event candidate
ATLAS
EXPERIMENT
Event Number: 00303638
Run Number: 05070508523
Date: 2016-07-11 11:54:14 CEST
pT_j1 =
301 GeV
pT_j3 =
40 GeV
pT_j2 =
261 GeV
pT_y2 =
130 GeV
pT_y1 =
339 GeV
m_jj = 482 GeV
m_yy = 125 GeV
pT_yy = 452 GeV

Measured differential cross sections

$|y_{\gamma\gamma}|$

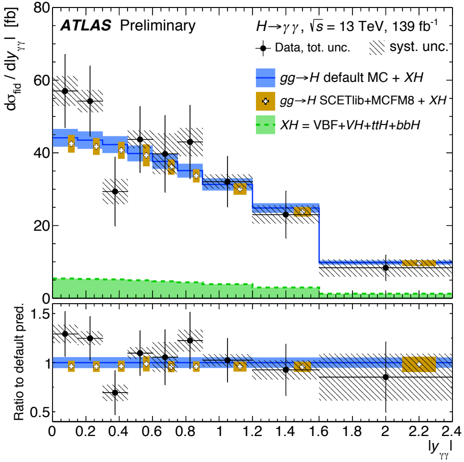

m_{jj}

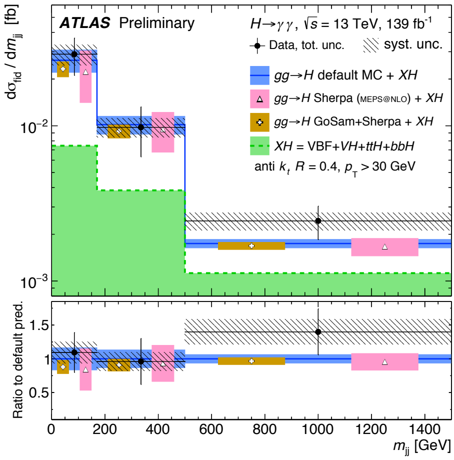

Measured differential cross sections

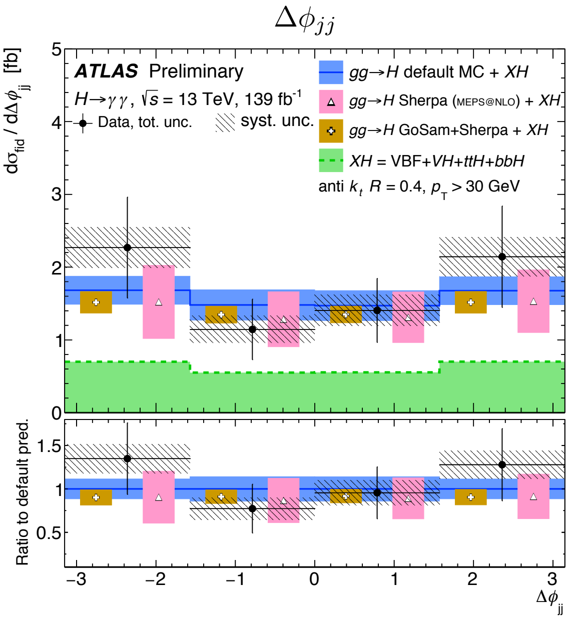

Vacuum metastability

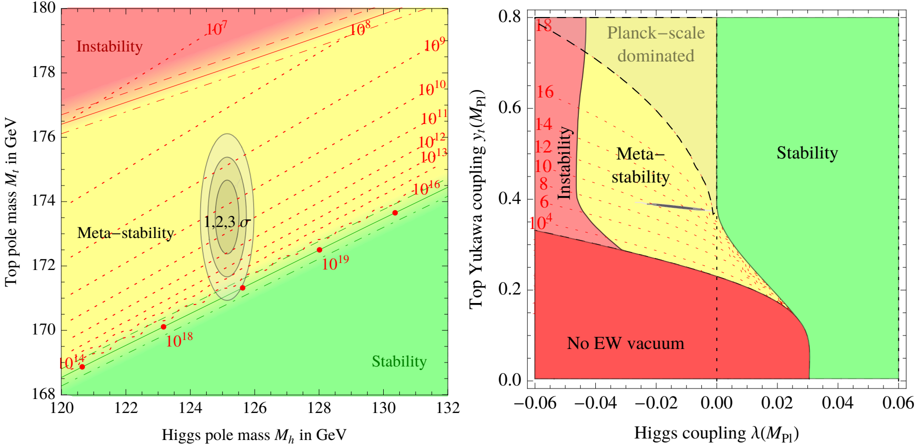

[arXiv:1307.3536]

Sketch of a hadron-hadron collision

as simulated by a typical Monte Carlo event generator program

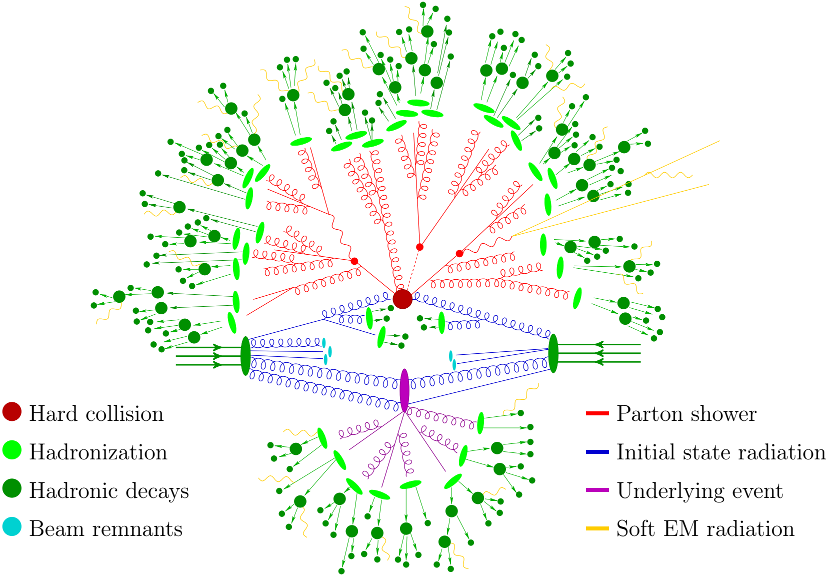

[30]

References I

[1] Illustration by a CERN artist. “Higgs for Waldegrave”. URL: http://www.hep.ucl.ac.uk/~djm/higgsa.html.

[2] K. Jepsen. “Famous Higgs analogy, illustrated”. *Symmetry magazine* (June 2013). URL: https://www.symmetrymagazine.org/article/september-2013/famous-higgs-analogy-illustrated.

[3] P. A. Zyla et al., Particle Data Group. “Review of Particle Physics”. *PTEP* 8 (2020), 083C01. DOI: 10.1093/ptep/ptaa104. cds: 2729066.

[4] LHC Higgs Cross Section Working Group. *Handbook of LHC Higgs Cross Sections: 3. Higgs Properties*. 2013. doi: 10.5170/CERN-2013-004. arXiv: 1307.1347. cds: 1559921.

[5] R. Tanaka, LHC Higgs Cross Section Working Group. Jan. 2011. url: https://twiki.cern.ch/twiki/bin/view/LHCPhysics/CrossSections.

[6] ATLAS Collaboration. “Observation of a new particle in the search for the Standard Model Higgs boson with the ATLAS detector at the LHC”. *Phys. Lett. B* **716** (Aug. 2012), 1–29. doi: 10.1016/j.physletb.2012.08.020. arXiv: 1207.7214. cds: 1471031.

[7] CMS Collaboration. “Observation of a new boson at a mass of 125 GeV with the CMS experiment at the LHC”. *Phys. Lett. B* **716** (Aug. 2012), 30. doi: 10.1016/j.physletb.2012.08.021. arXiv: 1207.7235. cds: 1471031.

[8] ATLAS Collaboration. “Observation of $H \to b\bar{b}$ decays and VH production with the ATLAS detector”. *Phys. Lett. B* **786** (Nov. 2018), 59–86. doi: 10.1016/j.physletb.2018.09.013. arXiv: 1808.08238. cds: 2636066. url: https://atlas.web.cern.ch/Atlas/GROUPS/PHYSICS/PAPERS/HIGG-2018-04/.

[9] ATLAS Collaboration. “Cross-section measurements of the Higgs boson decaying into a pair of τ-leptons in proton-proton collisions at $\sqrt{s} = 13$ TeV with the ATLAS detector”. *Phys. Rev. D* **99** (Apr. 2019), 072001. doi: 10.1103/PhysRevD.99.072001. arXiv: 1811.08856. cds: 2648520.

[10] ATLAS Collaboration. “A search for the dimuon decay of the Standard Model Higgs boson with the ATLAS detector”. (July 2020). arXiv: 2007.07830. cds: 2724102. url: https://atlas.web.cern.ch/Atlas/GROUPS/PHYSICS/PAPERS/HIGG-2019-14.

References II

[11] CMS Collaboration. “Measurement of Higgs boson decay to a pair of muons in proton-proton collisions at $\sqrt{s} = 13$ TeV”. CMS-PAS-HIG-19-006. 2020. cds: 2725423.

[12] Service graphique, CERN. “Overall view of the LHC”. June 2014. cds: 1708849.

[13] J. Pequenão. “Computer generated image of the whole ATLAS detector”. CERN-GE-0803012. Mar. 2008. cds: 1095924.

[14] J. Pequenão. “Event Cross Section in a computer generated image of the ATLAS detector.” CERN-GE-0803022. Mar. 2008. cds: 1096081.

[15] ATLAS Collaboration. *ATLAS calorimeter performance: Technical Design Report*. Technical Design Report ATLAS CERN-LHCC-96-040. 1996. cds: 331059.

[16] ATLAS Collaboration. “Measurements and interpretations of Higgs-boson fiducial cross sections in the diphoton decay channel using 139 fb^{-1} of pp collision data at $\sqrt{s} = 13$ TeV with the ATLAS detector”. ATLAS-CONF-2019-029. July 2019. cds: 2682800. url: https://atlas.web.cern.ch/Atlas/GROUPS/PHYSICS/CONFNOTES/ATLAS-CONF-2019-029/.

[17] HSG1 Group, ATLAS Collaboration. “Measurement of fiducial and differential cross sections in the $H \to \gamma\gamma$ decay channel with 140 fb^{-1} of 13 TeV proton–proton collision data with the ATLAS detector”. ATL-COM-PHYS-2019-035. Jan. 2019. cds: 2654897.

[18] C. Anastasiou et al. “Higgs Boson Gluon-Fusion Production in QCD at Three Loops”. *Phys. Rev. Lett.* **114** (May 2015), 212001. doi: 10.1103/PhysRevLett.114.212001. arXiv: 1503.06056.

[19] ATLAS Collaboration. “Combined measurement of the total and differential cross sections in the $H \to \gamma\gamma$ and the $H \to ZZ^* \to 4\ell$ decay channels at $\sqrt{s} = 13$ TeV with the ATLAS detector”. In: *EPS-HEP2019*. ATLAS-COM-CONF-2019-049. July 2019. cds: 2681143.

References III

[20] S. Laplace et al., ATLAS Collaboration. “Measurement of the Higgs boson production cross section at 7, 8 and 13 TeV center-of-mass energies in the $H \to \gamma\gamma$ channel with the ATLAS detector”. ATLAS-CONF-2015-060. Dec. 2015. cds: 2114826. url: https://atlas.web.cern.ch/Atlas/GROUPS/PHYSICS/CONFNOTES/ATLAS-CONF-2015-060/.

[21] HSG1 Group, ATLAS Collaboration. “Measurement of the fiducial cross section of the Higgs boson in the diphoton decay channel using 13 TeV pp data”. ATL-COM-PHYS-2015-1244. Oct. 2015. cds: 2056804.

[22] ATLAS Collaboration. “Measurement of fiducial, differential and production cross sections in the $H \to \gamma\gamma$ decay channel with 13.3 fb^{-1} of 13 TeV proton-proton collision data with the ATLAS detector”. ATLAS-CONF-2016-067. Aug. 2016. cds: 2206210. url: https://atlas.web.cern.ch/Atlas/GROUPS/PHYSICS/CONFNOTES/ATLAS-CONF-2016-067/.

[23] HSG1 Group, ATLAS Collaboration. “Measurement of the fiducial and differential cross sections of the Higgs boson in the diphoton decay channel using 2015/2016 13 TeV pp data”. ATL-COM-PHYS-2016-433. May 2016. cds: 2150683.

[24] ATLAS Collaboration. “Measurements of Higgs boson properties in the diphoton decay channel with 36.1 fb^{-1} pp collision data at the center-of-mass energy of 13 TeV with the ATLAS detector”. ATLAS-CONF-2017-045. July 2017. cds: 2273852. url: https://atlas.web.cern.ch/Atlas/GROUPS/PHYSICS/CONFNOTES/ATLAS-CONF-2017-045/.

[25] ATLAS Collaboration. “Measurements of Higgs boson properties in the diphoton decay channel with 36 fb^{-1} of pp collision data at $\sqrt{s} = 13$ TeV with the ATLAS detector”. *Phys. Rev. D* **98** (Sept. 2018), 052005. doi: 10.1103/PhysRevD.98.052005. arXiv: 1802.04146. url: https://atlas.web.cern.ch/Atlas/GROUPS/PHYSICS/PAPERS/HIGG-2016-21/.

[26] HSG1 Group, ATLAS Collaboration. “Measurement of fiducial and differential cross sections in the $H \to \gamma\gamma$ decay channel with 36 fb^{-1} of 13 TeV proton-proton collision data with the ATLAS detector”. ATL-COM-PHYS-2017-145. Feb. 2016. cds: 2252597.

References IV

[27] ATLAS Collaboration. “Measurements of Higgs boson properties in the diphoton decay channel using 80 fb^{-1} of pp collision data at $\sqrt{s} = 13$ TeV with the ATLAS detector”. ATLAS-CONF-2018-028. July 2018. cds: 2628771. url: https://atlas.web.cern.ch/Atlas/GROUPS/PHYSICS/CONFNOTES/ATLAS-CONF-2018-028/.

[28] HSG1 Group, ATLAS Collaboration. “Measurement of fiducial and differential cross sections in the $H \to \gamma\gamma$ decay channel with 80 fb^{-1} of 13 TeV proton–proton collision data with the ATLAS detector”. ATL-COM-PHYS-2018-202. Mar. 2018. cds: 2306798.

[29] D. Buttazzo et al. “Investigating the near-criticality of the Higgs boson”. *JHEP* 12 (Dec. 2013), 089. doi: 10.1007/JHEP12(2013)089. arXiv: 1307.3536.

[30] S. Höche. “Introduction to parton-shower event generators”. (2014). arXiv: 1411.4085.